Laser–Ion Beam Photodissociation Studies of Ionic Cluster Fragments of Transition-Metal Carbonyls

R. E. Tecklenburg, Jr., and D. H. Russell*

Contribution from the Department of Chemistry, Texas A&M University, College Station, Texas 77840. *Received March 11, 1987*

Abstract: Ionic cluster fragments of the type $M_x(CO)_y^+$ are studied by laser–ion beam photodissociation. The systems studied include $Mn_x(CO)_y^+$ (x = 1–2; y = 0–10, derived from $Mn_2(CO)_{10}$), $Fe_x(CO)_y^+$ (x = 3; y = 5–12, derived from $Fe_3(CO)_{12}$), and $Co_x(CO)_y^+$ (x = 2–4; y = 0–12, derived from $Co_4(CO)_{12}$). Relative photodissociation cross sections for each ion and upper limits to bond dissociation energies for M–M and M–CO are reported. Average metal–metal bond energies for the $Mn_2(CO)_y^+$ and $Co_4(CO)_y^+$ ions are found to be <44 and 16 kcal/mol, respectively. M–M bond energies could not be determined for $Fe_3(CO)_y^+$ ions because photodissociation of this system is dominated by expulsion of the CO ligand. Upper limits for metal–ligand bond energies determined are <25, 24, and 23 kcal/mol for $Mn_2(CO)_y^+$, $Fe_3(CO)_y^+$, and $Co_4(CO)_y^+$ systems, respectively.

The structure(s) of gas-phase ionic cluster fragments of transition-metal carbonyls and structure/reactivity relationships[1-4] are questions of current fundamental interest. Questions regarding structure/reactivity relationships for gas-phase ionic systems are difficult to probe experimentally. The more conventional mass spectrometric structural characterization methods (e.g., collision-induced dissociation) are inadequate because the only fragment ions observed correspond to loss of the carbonyl ligands.[3] In more complex systems, such as metal ion clusters and/or metal ion clusters containing complex organic ligands, C–H and C–C metal ion insertion reactions occur, thus leading to structural rearrangements.[5-7] To date the most successful approaches for probing structure/reactivity relationships have been based on the analysis of kinetic data.[4] In this paper the preliminary results for laser–ion beam photodissociation studies of ionic cluster fragments of transition-metal carbonyls are presented.

Mass spectrometry techniques provide important information on the chemistry and physical properties of novel transition-metal species. The chemistry of ionic transition-metal species is a rapidly growing field. For example, ionic clusters have been studied by single photon[8-10] and multiphoton[11-13] ionization/dissociation methods, as well as by ion–molecule reactions.[1-4,14-17] Fourier transform mass spectrometry (FTMS) is especially useful for studying ion/neutral interactions and has been used for probing structures of some simple transition-metal ions produced by ion–molecule reactions.[16,18-20] Thermodynamic information on transition-metal compounds and cluster ions has been obtained by numerous experimental techniques and various types of mass spectrometers, e.g., adiabatic and vertical ionization potentials,[8] appearance potentials,[21] gas-phase basicities,[15] proton affinities,[22] anion affinities,[23] electron affinities by photodetachment methods,[24-26] bond dissociation energies measured from collision-induced dissociation,[16,19,20] and threshold photodissociation measurements.[19,22,27,28]

Photodissociation methods are potentially quite useful for characterization of ionic transition-metal clusters, especially for estimates of metal–metal and metal–ligand bond energies and electron affinities.[20,28-32] To date most photodissociation work on transition-metal systems has been performed by ion cyclotron resonance (ICR) and time of flight (TOF) mass spectrometry. A problem with these methods, however, is that the ions are in the presence of neutral atoms or molecules for long periods of time, thus the photodissociation studies may be complicated by the occurrence of ion–molecule reactions. Another problem with the TOF multiphoton ionization/dissociation experiment is that photodissociation of the neutral can precede ionization. If the photofragment neutral is reactive it may recombine with other species and subsequently be ionized by MPI. Hence, elucidation of specific precursor–product ion pathways can be difficult.

Laser–ion beam photodissociation techniques provide an alternative to TOF and ICR photodissociation methods. Specifically, the ions are produced in the ion source, collimated into a beam, extracted into a field-free region, and irradiated with a high-intensity photon beam. Product ions formed by photodissociation are subsequently mass analyzed. Because ion formation and photodissociation occur in different regions of the mass spectrometer which are differentially pumped by individual vacuum

(1) Anderson Fredeen, D. J.; Russell, D. H. *J. Am. Chem. Soc.* **1985**, *107*, 3762.
(2) Anderson Fredeen, D. J.; Russell, D. H. *J. Am. Chem. Soc.* **1986**, *108*, 1860.
(3) Anderson Fredeen, D. J.; Russell, D. H. *J. Am. Chem. Soc.*, in press.
(4) Wronka, J.; Ridge, D. P. *J. Am. Chem. Soc.* **1984**, *106*, 67.
(5) Hettich, R. L.; Freiser, B. S. *J. Am. Chem. Soc.* **1987**, *109*, 3537.
(6) Hettich, R. L.; Freiser, B. S. *J. Am. Chem. Soc.* **1987**, *109*, 3543.
(7) Boo, B. H.; Armentrout, P. B. *J. Am. Chem. Soc.* **1987**, *109*, 3549.
(8) Lloyd, D. R.; Schlag, E. W. *Inorg. Chem.* **1969**, *8*, 2544.
(9) Jacobson, D. B. Freiser, B. S. *J. Am. Chem. Soc.* **1983**, *105*, 7484.
(10) Vaida, V.; Cooper, N. J.; Hemley, R. J.; Leopold, D. G. *J. Am. Chem. Soc.* **1981**, *103*, 7022.
(11) Leopold, D. G.; Vaida, V. *J. Am. Chem. Soc.* **1983**, *105*, 6809.
(12) Harrison, W. W.; Rider, D. M.; Zare, R. N. *Int. J. Mass. Spectrom. Ion Proc.* **1985**, *65*, 59.
(13) Carlin, T. J.; Freiser, B. S. *Anal. Chem.* **1983**, *55*, 955.
(14) Armentrout, P. B.; Beauchamp, J. L. *J. Am. Chem. Soc.* **1981**, *103*, 6628.
(15) Foster, M. S.; Beauchamp, J. L. *J. Am. Chem. Soc.* **1975**, *97*, 4808.
(16) Jacobson, D. B.; Freiser, B. S. *J. Am. Chem. Soc.* **1986**, *108*, 27.
(17) Foster, M. S.; Beauchamp, J. L. *J. Am. Chem. Soc.* **1971**, *93*, 4924.
(18) Russell, D. H.; Bricker, D. L. *Anal. Chim. Acta* **1985**, *178*, 117.
(19) Hettich, R. L.; Freiser, B. S. *J. Am. Chem. Soc.* **1985**, *107*, 6222.
(20) Jacobson, D. B.; Freiser, B. S. *J. Am. Chem. Soc.* **1984**, *106*, 4623.
(21) Conard, B. R.; Sridhar, R. *Can. J. Chem.* **1978**, *56*, 2607.
(22) Cassady, C. J.; Freiser, B. S. *J. Am. Chem. Soc.* **1984**, *106*, 6176.
(23) Lane, K. R.; Sallans, L.; Squires, R. R. *J. Am. Chem. Soc.* **1985**, *107*, 5369.
(24) Lineberger, W. C. *J. Am. Chem. Soc.* **1979**, *101*, 5569.
(25) Stevens, A. E.; Feigerle, C. S.; Lineberger, W. C. *J. Am. Chem. Soc.* **1982**, *104*, 5026.
(26) Zheng, L. S.; Brucat, P. J.; Pettiette, C. L.; Yang, S.; Smalley, R. E. *J. Chem. Phys.* **1985**, *83*, 4273.
(27) Brucat, P. J.; Zheng, L. S.; Pettiette, C. L.; Yang, S.; Smalley, R. E. *J. Chem. Phys.* **1986**, *84*, 3078.
(28) Hettich, R. L.; Jackson, T. C.; Stanko, E. M.; Freiser, B. S. *J. Am. Chem. Soc.* **1986**, *108*, 5086.
(29) Richardson, J. H.; Stephenson, L. M.; Brauman, J. I. *J. Am. Chem. Soc.* **1974**, *96*, 3671.
(30) Rynard, C. M.; Brauman, J. I. *Inorg. Chem.* **1980**, *19*, 3544.
(31) Dunbar, R. C. *Gas Phase Ion Chemistry*; Bowers, M. T., Ed.; Academic: New York, 1979; Vol. 2, p 181.
(32) Dunbar, R. C. *Molecular Ions: Spectroscopy, Structure and Chemistry*; Miller, T., A., Bondybey, V. E., Eds.; North-Holland: Amsterdam, 1983; p 231.

0002-7863/87/1509-7654$01.50/0

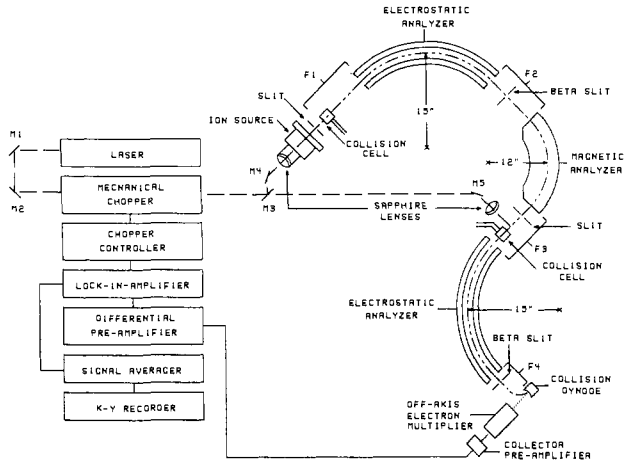

Figure 1. Schematic diagram of the laser–ion beam photodissociation apparatus. The laser beam (dashed line) is either directed toward the first field free region, F1 (coaxial experiment), or the third field free region, F3 (cross-beam experiment).

systems, interference from neutrals and recombination reactions are eliminated. Also, in the laser–ion beam photodissociation experiments, the laser beam is modulated by a mechanical chopper and the photodissociation signal for a specific process, i.e., $A^+ \rightarrow B^+ + C$ is measured in phase with the laser modulation. Thus, interferences and background signals, e.g., metastable and collision-induced dissociation reactions, are eliminated.

One of the goals of our research is to produce ionic transition-metal cluster fragments by ion–molecule reactions in a high-pressure ion source and investigate the photochemistry and energetics of dissociation of these ions under the single-photon photodissociation conditions.[1-3] To test the feasibility of such studies, this paper presents the results of photodissociation studies of ionic cluster fragments formed by direct electron impact ionization of stable transition-metal carbonyls of manganese, iron, and cobalt, i.e., $Mn_2(CO)_{10}$, $Fe_3(CO)_{12}$, and $Co_4(CO)_{12}$.

Experimental Section

A schematic diagram of the experimental apparatus used for the laser–ion beam photodissociation studies is shown in Figure 1. The apparatus consists of a triple analyzer Kratos MS-50 TA mass spectrometer, a Coherent CR-18 continuous wave argon ion laser, a Coherent CR-599 dye laser, and components for performing phase-sensitive detection. A similar apparatus and the laser–ion beam photodissociation experiments have been described elsewhere.[33] Six different wavelengths from the argon ion laser are used to measure photodissociation cross sections (457.9, 476.5, 488.0, 496.5, 501.7, 514.5 nm). In addition, when 3 W of λ = 514.5 nm is used to pump rhodamine 590 chloride dye, the dye laser produces a continuum of wavelengths over the range 550–675 nm. In the present study seven wavelengths of the dye laser are used (581, 592.5, 604, 616, 627.7, 640, 651 nm).

Ions are produced in an electron impact (EI) source with an ionizing energy of 70 eV. The Kratos MS-50 TA is designed so that photoinduced reactions occurring in both the first field free region (accelerating voltage (V) scans) and in the third field free region (mass analyzed ion kinetic energy (MIKE) scans) can be monitored. However, all experiments described herein are performed by using V scans.[33] In these experiments the laser beam is directed through the ion source and aligned coaxially with the ion beam in the first field free region of the mass spectrometer, by use of a series of mirrors and a 300 mm focal length sapphire focusing lens. The laser beam enters a modified EI source through a 1.75-cm sapphire window mounted on the source flange and passes through a 2-mm hole in the source repeller plate before entering the first field free region. The laser beam is mechanically chopped at a frequency of 400 Hz, and the photoinduced signal is separated from metastable and collision-induced products by using a lock-in amplifier (Princeton Applied Research Model 124A) which measures the laser "on"/laser "off" difference signal. The difference signal is then accumulated and signal-averaged with a Model 1170 Nicolet signal averager. Typically, 16 scans are signal averaged to produce photodissociation spectra. However, in some cases the measured photodissociation signal is small (due to either a small absorption cross section or low laser power) and a reasonable signal-to-noise ratio requires 32 scans (or more) to be signal-averaged. The stored-averaged spectra are then plotted by using a Houston Instrument Series 2000 X–Y recorder. Laser alignment is accomplished by adjusting the micrometer screws on the mirror mounts until the optimum photodissociation signal is achieved for loss of two carbonyl ligands from $Fe(CO)_4^+$ (476.5 nm) or loss of Cl from benzyl chloride (604 nm). Laser powers are measured by a Model 210 Coherent power meter.

There are two potential problems associated with coaxial photodissociation measurements as described above. (i) Because the laser beam passes through the ion source it is possible that an ion will absorb a photon while in the ion source (ion source residence time ca. 1×10^{-6} s) and dissociate after entering the first field free region ($2-5 \times 10^{-6}$ s following ion formation) of the mass spectrometer. (ii) Although the ion source and first field free regions are differentially pumped, there is a finite gas conductance between these two regions of the mass spectrometer. Thus, gas leakage between the ion source and first field free region could increase the pressure in the analyzer and increase the background collision-induced dissociation signal.[34] The relative importance of processes i and ii were estimated by performing photodissociation measurements at different repeller voltage settings, which alters the ion source residence times by as much as ten times,[35,36] and monitoring the photodissociation signal as a function of the ion source pressure. Varying either of these parameters does not result in a significant change in the photodissociation data. To minimize the effects of processes i and ii on the photodissociation data, all measurements reported herein were made in the following manner: (1) repeller voltage settings were chosen to minimize the ion source residence time and maximize the ion collector signal, and (2) minimum ion source pressures were used such that adequate signal-to-noise ratios were obtained without making the data acquisition times unreasonable.

When laser and ion beams are perfectly aligned coaxially, a field free interaction distance of 15 to 20 cm is obtainable. It should be pointed out that for both ranges of wavelengths used (458–514.5 and 581–651 nm), photodissociation cross sections are calculated by assuming identical overlaps between the coaxially aligned laser and ion beams in the first field free region of the mass spectrometer. Since there is no way of estimating how similar the overlaps for the two experiments are, no corrections are made in the cross-section calculations (see Results section).

$Fe_3(CO)_{12}$ and $Co_4(CO)_{12}$ were purchased from Strem Chemical, Inc. (Newburyport MA 01950), while $Fe(CO)_5$ was purchased from Alpha Products Thiokol/Ventron Division (Danvers, MA 01953). Rhodamine 590 chloride dye was purchased from Exciton Chemical Co., Inc. (Dayton, OH, 45431). The samples were introduced into the mass spectrometer by either a direct insertion liquids probe or a direct insertion solids probe. The ion source and insertion probes were not heated since heating from the source filament to the source block was sufficient ($\sim$ 100 °C) to adequately sublime the samples. Since no measureable impurities were observed in the mass spectra of these compounds, the samples were used without further purification.

Results

This work investigates the visible single-photon photodissociation of transition-metal fragment ions formed by electron-impact ionization and subsequent fragmentation of $Mn_2(CO)_{10}$, $Fe_3(CO)_{12}$, and $Co_4(CO)_{12}$. The 70 eV electron impact ionization mass spectra of $Mn_2(CO)_{10}$, $Fe_3(CO)_{12}$, and $Co_4(CO)_{12}$ have previously been reported.[37-39] At 70 eV ionizing energy, Mn_2^+ and Mn^+ are found to be the most abundant ions in the electron impact mass spectrum of $Mn_2(CO)_{10}$. For $Fe_3(CO)_{12}$, rupture

(33) Krailler, R. E.; Russell, D. H.; Jarrold, M. F.; Bowers, M. T. *J. Am. Chem. Soc.* **1985**, *107*, 2346.

(34) A referee has suggested that product ions of photodissociation (photofragment ions) may recombine with neutrals in the first field free region as a result of the high neutral pressure. If this were to occur the signal for the product of the photofragment ion/neutral reaction would occur synchronously with the laser modulation. It is unlikely, however, that photofragment ion/neutral recombination reactions would occur because of the high velocity of the ion. Note also that collision-induced dissociation as a result of gas conductance between the two vacuum regions would be continuous and would not be phase related to the laser modulation.

(35) Sellers-Hahn, L.; Russell, D. H. *J. Chem. Phys.*, submitted for publication.

(36) Morgan, T. G.; March, R. E.; Harris, F. M.; Beynon, J. H. *Int. J. Mass Spectrom. Ion Proc.* **1984**, *61*, 41.

(37) Winters, R. E.; Kiser, R. W. *J. Phys. Chem.* **1965**, *69*, 1618.

(38) Lewis, J.; Manning, A. R.; Miller, J. R.; Wilson, J. M. *J. Chem. Soc. A* **1966**, 1663.

(39) Johnson, B. F. G.; Lewis, J.; Williams, I. G.; Wilson, J. M. *J. Chem. Soc. A* **1967**, 341.

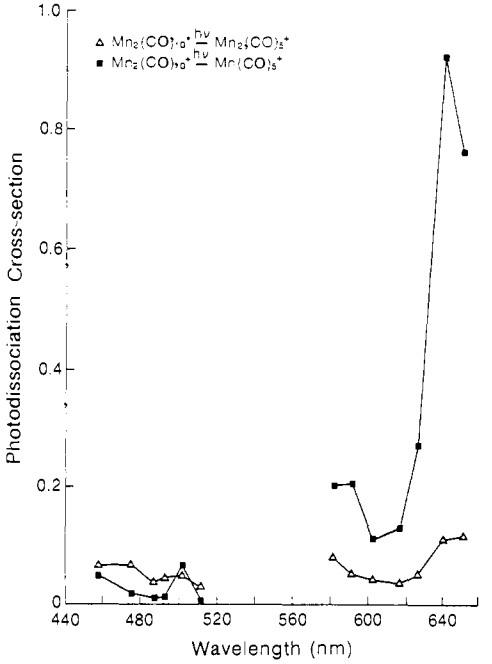

Figure 2. Photofragment ion yield as a function of laser wavelength for $Mn_2(CO)_{10}^+$. The photofragment ions are $Mn_2(CO)_5^+$ (Δ) and $Mn(CO)_5^+$ (■).

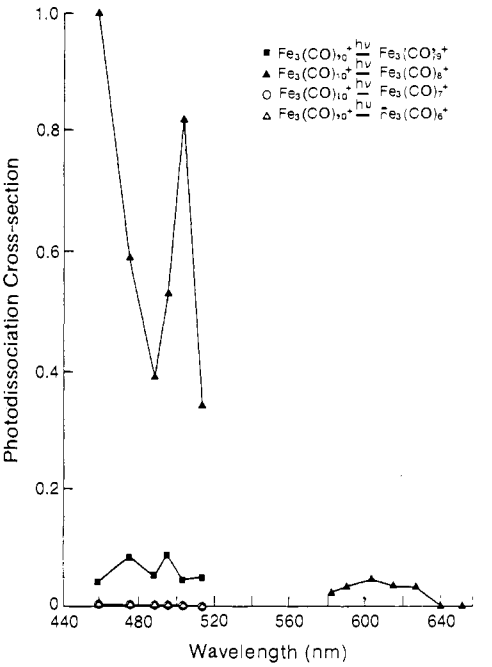

Figure 3. Photofragment ion yield as a function of laser wavelength for $Fe_3(CO)_{10}^+$. The photofragment ions are $Fe_3(CO)_9^+$ (■), $Fe_3(CO)_8^+$ (▲), $Fe_3(CO)_7^+$ (○), and $Fe_3(CO)_6^+$ (△).

of all metal carbonyl bonds to produce Fe_3^+ is possible. Fe–Fe bonds of $Fe_3(CO)_{12}$ are also easily broken upon electron impact ionization, and at m/z values less than 280, di- and mono-iron carbonyl species are also observed. Mass doublets (m/z = 280, 252, 224, 140, 112) and triplets (m/z = 196, 168) are observed in the high-resolution mass spectrum of $Fe_3(CO)_{12}$, e.g., m/z = 168 corresponds to $Fe(CO)_4^+$, $Fe_2(CO)_2^+$, and Fe_3^+ ions. These mass doublets and triplets require a resolution of 4000–5000 for base line separation of the individual ions. Although the mass doublets can be resolved in the normal magnet scan spectrum, the mass resolution for first field free region decomposition scan methods is not adequate for complete resolution. Consequently, the present study will be limited to the photodissociation of $Fe_3(CO)_y^+$ ions where mass overlap does not occur ($y \geq 5$). For $Co_4(CO)_{12}$, the most intense peak in the electron impact mass spectrum is $Co_4(CO)_7^+$. Even though metal–carbonyl and metal–metal bond strengths are greater for this compound than for $Fe_3(CO)_{12}$, the bare metal ions Co_4^+, Co_3^+, Co_2^+, and Co^+ are observed in the 70 eV mass spectrum.

Two wavelength ranges of the laser are used to examine photodissociation reactions occurring in the first field free region of the mass spectrometer. Six wavelengths from the argon ion laser (458–514.5 nm), which vary in power from 1 to 10 W, and seven wavelengths (100–800 mW) from the Coherent CR-599 rhodamine 6G dye laser (581–651 nm) are used.

Relative photodissociation cross sections are calculated for all photodissociating ions as a function of laser wavelength. Photodissociating ions are organized into three tables according to the neutral species from which each is produced. Tables I–III list all of the observed photodissociation reactions and the relative photodissociation cross sections at each wavelengths for $Mn_x(CO)_y^+$ (x = 1–2; y = 0–10), $Fe_x(CO)_y^+$ (x = 3; y = 5–12), and $Co_x(CO)_y^+$ (x = 2–4; y = 0–12) species, respectively. The relative photodissociation cross sections are normalized by using the following relationship

$$\sigma_{s(\lambda_1),r(\lambda_0)} = \frac{P_{r(\lambda_0)}}{P_{s(\lambda_1)}} \frac{RA_r}{RA_s} \frac{H_{s(\lambda_1)}}{H_{r(\lambda_0)}} \frac{G_{s(\lambda_1)}}{G_{r(\lambda_0)}}$$

where s and r denote the sample and reference transition, respectively; $\sigma_{s(\lambda_1),r(\lambda_0)}$ is the photodissociation cross section of sample transition s at λ_1 relative to the reference transition r at λ_0; P represents the laser power; RA is the relative ion abundance at the collector; H is the photofragment peak height; the G is the

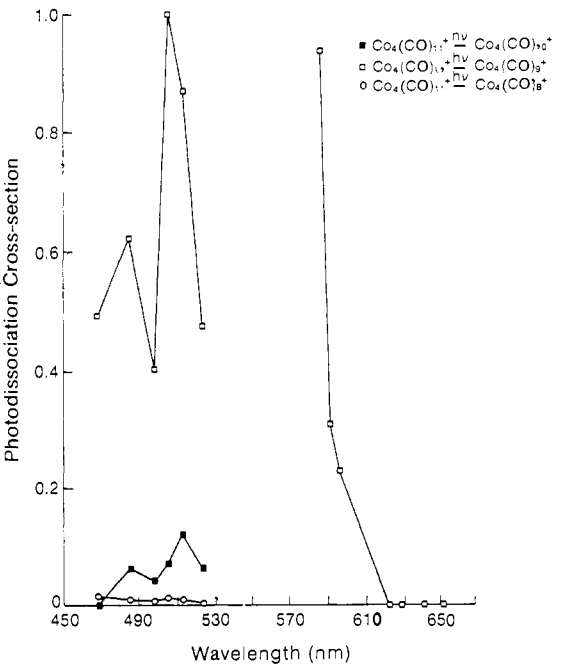

Figure 4. Photofragment ion yield as a function of laser wavelength for $Co_4(CO)_{11}^+$. The photofragment ions are $Co_4(CO)_{10}^+$ (■), $Co_4(CO)_9^+$ (□), and $Co_4(CO)_8^+$ (○).

signal averager gain used to record the photodissociation spectra. Photodissociation cross section measurements for each type of metal cluster system are normalized to the photodissociation reaction having the largest cross section. For example, in Table I loss of two carbonyl ligands from $Mn(CO)_5^+$ is found to have the largest relative photodissociation cross section at λ = 640 nm, and this reaction is assigned a photodissociation cross section of 1.00. Therefore, all the other photodissociating $Mn_x(CO)_y^+$ ions are normalized to this transition. Estimates of maximum uncertainty in the measured cross section values varied from 15% in the wavelength range 458–514.5 nm to 20% in the 581–651 nm wavelength range.

Selected photodissociation spectra for the Mn, Fe, and Co systems are plotted in Figures 2, 3, and 4, respectively. Photo-

Table I. Photodissociation Cross Sections Measured for $Mn_x(CO_y)^+$ Ions over the Wavelength Ranges 458–514 and 581–651 nm

Precursor Ion	Photofragment Ion	Wavelength (nm) 458	476	488	496	502	514	581	592	604	616	628	640	651
$Mn_2(CO)_{10}^+$	$Mn_2(CO)_5^+$	0.076	0.074	0.040	0.045	0.053	0.026	0.089	0.050	0.042	0.037	0.057	0.12	0.14
	$Mn(CO)_5^+$	0.059	0.021	0.014	0.017	0.077	0.0097	0.20	0.21	0.12	0.13	0.27	0.93	0.77
$Mn_2(CO)_9^+$	$Mn_2(CO)_5^+$	0.0059	0.0041	0.0025	0.0003	0.0034	0.0018	0.0046	0.0074	0.011	0.0096	0.0064	—	—
$Mn_2(CO)_7^+$	$Mn_2(CO)_5^+$	—	0.0010	0.0006	0.0009	—	0.0007	—	—	—	—	—	—	—
$Mn_2(CO)_6^+$	$Mn_2(CO)_5^+$	0.014	0.015	0.013	0.0095	0.015	0.011	0.049	0.027	0.021	0.035	0.026	0.051	0.046
$Mn_2(CO)_5^+$	$Mn_2(CO)_3^+$	0.048	0.048	0.033	0.027	0.037	0.014	0.24	0.43	0.30	0.24	0.20	0.15	0.11
	$Mn_2(CO)_2^+$	0.031	0.029	0.021	0.016	0.0099	0.016	0.0088	0.0064	0.0039	0.0037	0.013	0.024	0.032
	Mn_2^+	0.0009	0.0020	—	0.0003	0.0010	0.0001	0.0005	0.0009	0.0017	0.0051	0.0013	0.030	0.049
$Mn_2(CO)_4^+$	$Mn_2(CO)_2^+$	0.056	0.16	0.10	0.20	0.13	0.12	0.78	0.69	0.68	0.63	0.31	0.30	0.25
	$Mn_2(CO)^+$	0.16	0.13	0.28	0.16	0.25	0.16	0.30	0.26	0.17	0.078	0.078	0.058	0.028
	Mn_2^+	0.015	0.038	0.015	0.013	0.014	0.014	0.0005	0.0021	0.0070	0.0029	0.0033	0.049	0.044
	$Mn(CO)_3^+$	0.0053	0.016	0.019	0.020	0.023	0.030	0.095	0.066	0.063	0.071	0.15	0.29	0.33
$Mn_2(CO)_3^+$	$Mn_2(CO)^+$	0.0065	0.0031	0.0043	0.0018	0.011	0.0036	0.053	0.046	0.074	0.019	0.096	0.093	0.079
	Mn_2^+	0.014	0.035	0.016	0.015	0.013	0.017	0.043	0.041	0.037	0.041	0.049	0.040	0.035
$Mn_2(CO)_2^+$	$Mn_2(CO)^+$	0.028	0.010	0.020	0.020	0.045	0.014	0.12	0.064	0.074	0.061	0.069	0.28	0.23
	Mn_2^+	0.0040	0.010	0.0052	0.0046	0.0043	0.0048	0.029	0.044	0.039	0.034	0.037	0.069	0.081
$Mn_2(CO)^+$	Mn_2^+	0.0022	0.0051	0.0016	0.0020	0.0021	0.0010	0.0082	0.0061	0.012	0.011	0.029	0.024	0.018
	Mn^+	0.0011	0.0001	0.0006	0.0004	0.0005	—	—	—	—	—	—	—	—
Mn_2^+	Mn^+	0.027	0.023	0.019	0.017	0.022	0.035	0.047	0.034	0.0092	0.18	0.022	0.062	0.079
$Mn(CO)_5^+$	$Mn(CO)_3^+$	0.017	0.0079	0.0055	0.0091	0.018	0.031	0.43	0.80	0.70	0.71	0.84	1.00	0.83
	$Mn(CO)^+$	0.0051	0.0031	0.0012	0.0014	0.0044	0.0008	—	—	—	—	—	—	—
$Mn(CO)_4^+$	$Mn(CO)_3^+$	0.030	0.012	0.0053	0.013	0.022	0.0068	—	—	—	—	—	—	—

dissociation of the $Mn_2(CO)_{10}^+$ ion (Figure 2) yields both $Mn_2(CO)_5^+$ and $Mn(CO)_5^+$ fragment ions in both the low- and high-energy regions of the visible spectrum. Both reactions have similar relative photodissociation cross sections at high energy, but formation of the $Mn(CO)_5^+$ ion dominates at low energies. The $Mn(CO)_5^+$ ion shows an apparent photodissociation maximum (0.926) at 640 nm. The relative photodissociation cross sections for this transition are typical of the manganese carbonyl ions: i.e., large photodissociation cross sections at low energies (581–651 nm) with much smaller photodissociation cross sections at high energies (458–514.5 nm). The fact that both $Mn(CO)_5^+$ and $Mn_2(CO)_5^+$ are formed by photodissociation of $Mn_2(CO)_{10}^+$ is interesting and perplexing. This observation is discussed further in the Discussion section.

Loss of two carbonyls from $Fe_3(CO)_{10}^+$ is found to have the largest photodissociation cross section (λ_{max} = 458 nm) (see Table II) for the $Fe_3(CO)_y^+$ ions. The photodissociation data for all photofragment product ions arising from $Fe_3(CO)_{10}^+$ are plotted in Figure 3. At long wavelengths ($\lambda \geq 581$ nm), loss of two carbonyls is the exclusive photodissociation reaction channel. At higher energies loss of one, three, and four CO ligands from $Fe_3(CO)_{10}^+$ is observed at low yield (10–1000 times less than that for loss of two CO ligands), but the photoproducts from these reactions are still rather easily detected since no significant background (metastable ions) arises to compete with the laser-induced signal. For $Fe_3(CO)_y^+$ ions it should be noted that the photodissociation cross section for $Fe_3(CO)_{10}^+$ to give $Fe_3(CO)_8^+$ is extremely large. Although the photodissociation cross sections for other $Fe_3(CO)_y^+$ ions are small relative to $Fe_3(CO)_{10}^+$, the photodissociation reactions are easily detected.

Loss of two CO groups from $Co_4(CO)_{11}^+$ (λ_{max} = 496 nm) is found to have the largest photodissociation cross section of all cobalt carbonyl fragment ions (in Table III and Figure 4). Figure 4 also gives the photofragment ion yield for $Co_4(CO)_{10}^+$ and $Co_4(CO)_8^+$ daughter ions from $Co_4(CO)_{11}^+$. Loss of one and three CO ligands from the $Co_4(CO)_{11}^+$ ion are only minor photodissociation reactions (<10%) at most wavelengths. The $Co_4(CO)_{11}^+$ ion, however, easily photodissociates to $Co_4(CO)_9^+$ at both low and high energy. Note that the photodissociation cross section drops sharply from 0.967 at λ = 581 nm to 0 at wavelengths greater than 616 nm.

In general, photodissociation cross sections for iron and cobalt cluster ions are found to be larger at higher energies, and the photodissociation cross section for many of the ionic cluster

Table II. Photodissociation Cross Sections Measured for $Fe_3(CO)_y^+$ Ions over the Wavelength Ranges 458–514 and 581–651 nm

Precursor Ion	Photofragment Ion	Wavelength (nm) 458	476	488	496	502	514	581	592	604	616	628	640	651
$Fe_3(CO)_{12}^+$	$Fe_3(CO)_{10}^+$	0.0043	0.0038	0.0028	0.0061	0.0067	0.0039	0.0082	0.0074	0.0099	0.012	0.011	0.0047	—
	$Fe_3(CO)_9^+$	0.066	0.063	0.043	0.071	0.051	0.028	—	—	—	—	—	—	—
$Fe_3(CO)_{11}^+$	$Fe_3(CO)_9^+$	0.015	0.022	0.021	0.039	0.045	0.024	—	—	—	—	—	—	—
	$Fe_3(CO)_8^+$	0.056	0.029	0.011	0.0045	—	—	—	—	—	—	—	—	—
$Fe_3(CO)_{10}^+$	$Fe_3(CO)_9^+$	0.041	0.083	0.050	0.085	0.048	0.041	—	—	—	—	—	—	—
	$Fe_3(CO)_8^+$	1.00	0.59	0.39	0.53	0.82	0.37	0.026	0.034	0.041	0.037	0.034	—	—
	$Fe_3(CO)_7^+$	0.0043	0.0034	0.0002	0.0018	0.0014	—	—	—	—	—	—	—	—
	$Fe_3(CO)_6^+$	0.0006	0.0001	0.0002	0.0001	0.0001	—	—	—	—	—	—	—	—
$Fe_3(CO)_9^+$	$Fe_3(CO)_8^+$	0.20	0.21	0.16	0.20	0.38	0.22	—	—	—	—	—	—	—
	$Fe_3(CO)_7^+$	0.0020	0.0036	0.0010	0.0024	0.0018	—	0.0013	0.0008	0.0009	0.0004	—	—	—
	$Fe_3(CO)_6^+$	0.0013	0.0002	0.0001	0.0003	0.0001	0.0001	—	—	—	—	—	—	—
$Fe_3(CO)_8^+$	$Fe_3(CO)_6^+$	0.010	0.0084	0.0060	0.0084	0.0064	0.0032	0.0004	0.0005	0.0004	—	—	—	—
	$Fe_3(CO)_5^+$	0.0042	0.0031	0.0022	0.0022	0.0018	0.0012	—	—	—	—	—	—	—
$Fe_3(CO)_7^+$	$Fe_3(CO)_5^+$	0.015	0.019	0.016	0.024	0.028	0.027	0.0043	0.0065	0.0050	0.0042	0.0027	0.0002	—
	$Fe_3(CO)_4^+$	0.054	0.064	0.038	0.020	0.041	0.0051	0.017	0.0084	0.0016	—	—	—	—
$Fe_3(CO)_6^+$	$Fe_3(CO)_4^+$	0.17	0.10	0.12	0.11	0.17	0.036	0.084	0.030	0.014	0.0066	—	—	—
$Fe_3(CO)_5^+$	$Fe_3(CO)_4^+$	0.022	0.018	0.024	0.032	0.048	0.017	0.039	0.017	0.0065	0.0083	—	—	—

fragments reaches a maximum at 496 or 502 nm. At lower photon energies, iron and cobalt carbonyl ions have relative photodissociation cross sections that are 10 to 100 times smaller, and in many cases, the photodissociation cross sections drop to zero at wavelengths greater than 616 nm. The reverse trend is found for $Mn_x(CO)_y^+$ ions. These ions have large photodissociation cross sections in the wavelength range 581–651 nm, and most of the $Mn_x(CO)_y^+$ cluster ions continue to photodissociate at the lowest energy wavelength (651 nm). Because metal–metal and metal–carbonyl bond strengths increase in the series Mn < Fe < Co, it is expected that the percentage of ions photodissociating at low energies will be greatest for $Mn_x(CO)_y^+$ ions. This is indeed found to be the case with 82% of the $Mn_x(CO)_y^+$ ions, 47% of the $Fe_3(CO)_y^+$ ions, and 30% of the $Co_x(CO)_y^+$ ions photodissociating at long wavelengths ($\lambda \geq 581$ nm).

It is interesting to note that most of the iron and cobalt ions, which photodissociate at low energy (581–651 nm) (see Tables II and III), undergo specific reactions corresponding to loss of two carbonyl ligands, exclusively. At higher energies (λ = 458–514.5 nm) these ions dissociate by loss of one, two, three, and four carbonyl ligands. We note this because such behavior is somewhat unusual. That is, the question arises concerning the observed loss of one carbonyl ligand at high energy when loss of three and four carbonyl ligands is energetically favorable. On the other hand, at low energy, loss of two CO's is observed and loss of one CO is not observed.

For those ions with photodissociation cross sections approaching zero above some critical wavelength, upper limits for metal–metal and metal–carbonyl bond strengths may be estimated.[40] The bond dissociation energies are obtained by dividing the photodissociation threshold energy (disappearance of a photodissociation signal) by the number of metal–metal and/or metal–ligand bonds ruptured. Tables IV–VI list the bond dissociation energies estimated for all $Mn_x(CO)_y^+$, $Fe_3(CO)_y^+$, and $Co_x(CO)_y^+$ ions.

Discussion

The photodissociation of transition-metal monomer and dimer ions has been studied in the ultraviolet,[19,28] but little is known about the single-photon photodissociation of ligated ionic transition-metal clusters in the visible. Freiser et al. suggested that the photodissociation of monomeric and dimeric ionic metal species is due to a virtual absorption continuum which arises from excitation via atomic-like electronic transitions.[19,22] Theoretical calculations indicate that dimeric metal species, via, Fe_2 and Co_2, possess high densities of low-lying electronic states.[41,42] If the density of states of these systems is extremely high, photodissociation should occur at virtually all wavelengths. However, a high density of low-lying excited electronic states is not consistent with the results of photodetachment studies. Lineberger and co-workers studied Fe_2 and Co_2 and reported a small number of discrete excited electronic states up to 1 eV above the ground electronic state.[43] Analogous to the observation reported by Lineberger, the ions listed in Tables I–III show distinct absorption bands. In fact, the absorption bands are similar to the absorption bands of their neutral counterparts. For example, compare the single-crystal absorption spectra of $Fe_3(CO)_{12}$ with the photodissociation spectra for $Fe_3(CO)_{12}^+ \rightarrow Fe_3(CO)_{10}^+$ shown in Figure 5. Note in both the neutral absorption and photodissociation spectra that strong bands are observed in the 500 and 620 nm wavelength regions.[44] Gray assigns

(40) The bond dissociation energy measured in this manner may be low if the ion being probed contains some excess internal energy.

(41) Shim, I.; Gingerich, K. A. *J. Chem. Phys.* **1982**, *77*, 2490.
(42) Lin, S. S.; Kant, A. *J. Phys. Chem.* **1969**, *73*, 2450.
(43) Leopold, D. G.; Lineberger, W. C. *J. Chem. Phys.* **1986**, *85*, 51.

Table III. Photodissociation Cross Sections Measured for $Co_x(CO)_y^+$ Ions over the Wavelength Ranges 458–514 and 581–651 nm

Precursor Ion	Photofragment Ion	Wavelength (nm) 458	476	488	496	502	514	581	592	604	616	628	640	651
$Co_4(CO)_{12}^+$	$Co_4(CO)_{10}^+$	0.39	0.52	0.34	0.64	0.58	0.36	0.73	0.59	0.32	0.36	0.31	—	—
	$Co_4(CO)_9^+$	0.15	0.10	0.053	0.096	0.051	0.021	—	—	—	—	—	—	—
	$Co_4(CO)_8^+$	0.0007	—	0.0025	0.0008	—	0.0024	—	—	—	—	—	—	—
$Co_4(CO)_{11}^+$	$Co_4(CO)_{10}^+$	—	0.035	0.022	0.073	0.12	0.062	—	—	—	—	—	—	—
	$Co_4(CO)_9^+$	0.49	0.62	0.41	1.00	0.87	0.47	0.97	0.32	0.23	—	—	—	—
	$Co_4(CO)_8^+$	0.019	0.015	0.0084	0.010	0.010	0.0045	—	—	—	—	—	—	—
$Co_4(CO)_{10}^+$	$Co_4(CO)_9^+$	0.75	0.74	0.46	0.96	0.93	0.46	—	—	—	—	—	—	—
	$Co_4(CO)_8^+$	0.043	0.043	0.042	0.046	0.041	0.042	—	—	—	—	—	—	—
$Co_4(CO)_9^+$	$Co_4(CO)_8^+$	0.11	0.065	0.038	0.061	0.067	0.029	—	—	—	—	—	—	—
	$Co_4(CO)_7^+$	0.0074	0.011	0.015	0.013	0.0099	0.010	—	—	—	—	—	—	—
$Co_4(CO)_8^+$	$Co_4(CO)_6^+$	0.045	0.11	0.063	0.090	0.097	0.092	0.049	0.050	0.065	0.095	—	—	—
	$Co_4(CO)_5^+$	0.073	0.050	0.024	0.021	0.023	0.0087	—	—	—	—	—	—	—
$Co_4(CO)_7^+$	$Co_4(CO)_5^+$	0.62	0.48	0.35	0.55	0.62	0.33	0.35	0.27	0.25	0.33	0.36	0.16	0.0083
	$Co_4(CO)_4^+$	0.42	0.21	0.14	0.11	0.13	0.081	—	—	—	—	—	—	—
$Co_4(CO)_6^+$	$Co_4(CO)_5^+$	0.024	0.048	0.071	0.097	0.12	0.060	—	—	—	—	—	—	—
	$Co_4(CO)_4^+$	0.19	0.17	0.17	0.15	0.21	0.16	0.039	0.077	0.10	0.18	0.085	0.051	0.0037
	$Co_4(CO)_3^+$	0.0062	0.0026	0.0019	0.0039	0.013	0.0012	—	—	—	—	—	—	—
$Co_4(CO)_5^+$	$Co_4(CO)_4^+$	0.16	0.10	0.087	0.083	0.12	0.065	—	—	—	—	—	—	—
	$Co_4(CO)_3^+$	0.020	0.014	0.012	0.017	0.13	0.014	0.027	0.035	0.021	0.016	0.016	—	—
$Co_4(CO)_4^+$	$Co_4(CO)_3^+$	0.015	0.011	0.011	0.0095	0.12	0.0099	—	—	—	—	—	—	—
	$Co_4(CO)_2^+$	0.012	0.011	0.0073	0.014	0.012	0.0084	—	—	—	—	—	—	—
$Co_4(CO)_3^+$	$Co_4(CO)_2^+$	0.021	0.022	0.014	0.022	0.020	0.017	—	—	—	—	—	—	—
	$Co_4(CO)^+$	0.0097	0.0074	0.0095	0.015	0.011	0.0042	0.011	0.016	0.0056	0.0050	0.0067	—	—
$Co_4(CO)_2^+$	$Co_4(CO)^+$	0.0089	0.0083	0.0071	0.011	0.014	0.0063	—	—	—	—	—	—	—
	Co_4^+	0.0074	0.0031	0.0021	0.0025	0.0052	0.0016	0.023	0.022	0.017	0.010	—	—	—
$Co_4(CO)^+$	Co_4^+	0.0083	0.0069	0.0040	0.0043	0.012	0.0035	—	—	—	—	—	—	—
	Co_3^+	0.11	0.053	0.037	0.034	0.14	0.020	—	—	—	—	—	—	—
Co_4^+	Co_3^+	0.081	0.065	0.052	0.045	0.12	0.044	0.036	0.024	—	—	—	—	—
	Co_2^+	0.0062	0.0024	0.0014	0.0016	0.0046	0.0007	—	—	—	—	—	—	—
Co_3^+	Co_2^+	0.017	0.0085	0.0061	0.0063	0.016	0.0061	—	—	—	—	—	—	—

the 500 and 620 nm transitions of the $Fe_3(CO)_{12}$ neutral species to the $\sigma \rightarrow \sigma^*$ and $\sigma^{*\prime} \rightarrow \sigma^*$ transitions and discounts the possibility of metal–ligand charge-transfer bands giving rise to electronic transitions in the visible spectral range. An interesting feature of the photodissociation spectrum is that the $\sigma \rightarrow \sigma^*$ (496–502 nm) band is red shifted by approximately 60–65 nm (0.36 eV) with respect to the neutral absorption spectrum. Such a red shift could indicate that the average splitting of the xz and z^2 orbitals differs for the ion, but it could also indicate that the ions sampled by photodissociation are vibrationally hot. More detailed studies aimed at answering these questions are underway.

In general, ionic transition-metal carbonyl cluster fragments readily photodissociate at visible wavelengths. The reason for this

(44) Tyler, D. R.; Levenson, R. A.; Gray, H. B. *J. Am. Chem. Soc.* **1978**, *100*, 7888.

Table IV. Bond Dissociation Energies Measured from Photodissociation Thresholds for $Mn_x(CO)_y^+$ Ions

TRANSITION	THRESHOLD		THRESHOLD ENERGY # BONDS BROKEN
	(nm)	(kcal/mole)	(kcal/mole)
$Mn_2(CO)_{10}^+ \longrightarrow Mn_2(CO)_6^+$	>651	<43.9	<8.8
$Mn_2(CO)_{10}^+ \longrightarrow Mn(CO)_5^+$	>651	<43.9	<43.9
$Mn_2(CO)_9^+ \longrightarrow Mn_2(CO)_6^+$	640	44.7	11.2
$Mn_2(CO)_6^+ \longrightarrow Mn_2(CO)_6^+$	>651	<43.9	<43.9
$Mn_2(CO)_5^+ \longrightarrow Mn_2(CO)_3^+$	>651	<43.9	<21.9
$Mn_2(CO)_6^+ \longrightarrow Mn_2(CO)_2^+$	>651	<43.9	<14.6
$Mn_2(CO)_6^+ \longrightarrow Mn_2(CO)^+$	>651	<43.9	<11.0
$Mn_2(CO)_4^+ \longrightarrow Mn_2(CO)_2^+$	>651	<43.9	<21.9
$Mn_2(CO)_4^+ \longrightarrow Mn_2(CO)^+$	>651	<43.9	<14.6
$Mn_2(CO)_4^+ \longrightarrow Mn_2^+$	>651	<43.9	<11.0
$Mn_2(CO)_4^+ \longrightarrow Mn(CO)_3^+$	>651	<43.9	<21.9
$Mn_2(CO)_3^+ \longrightarrow Mn_2(CO)^+$	>651	<43.9	<21.9
$Mn_2(CO)_3^+ \longrightarrow Mn_2^+$	>651	<43.9	<14.6
$Mn_2(CO)_2^+ \longrightarrow Mn_2(CO)^+$	>651	<43.9	<43.9
$Mn_2(CO)_2^+ \longrightarrow Mn_2^+$	>651	<43.9	<21.9
$Mn_2(CO)^+ \longrightarrow Mn_2^+$	>651	<43.9	<43.9
$Mn_2^+ \longrightarrow Mn^+$	>651	<43.9	<43.9
$Mn(CO)_6^+ \longrightarrow Mn(CO)_3^+$	>651	<43.9	<21.9

Table V. Bond Dissociation Energies Measured from Photodissociation Thresholds for $Fe_3(CO)_y^+$ Ions

TRANSITION	THRESHOLD		THRESHOLD ENERGY # BONDS BROKEN
	(nm)	(kcal/mole)	(kcal/mole)
$Fe_3(CO)_{12}^+ \longrightarrow Fe_3(CO)_{10}^+$	651	43.9	21.9
$Fe_3(CO)_{11}^+ \longrightarrow Fe_3(CO)_8^+$	502	56.9	18.9
$Fe_3(CO)_{10}^+ \longrightarrow Fe_3(CO)_8^+$	640	44.7	22.3
$Fe_3(CO)_9^+ \longrightarrow Fe_3(CO)_7^+$	628	45.5	22.8
$Fe_3(CO)_8^+ \longrightarrow Fe_3(CO)_6^+$	616	46.4	23.2
$Fe_3(CO)_7^+ \longrightarrow Fe_3(CO)_5^+$	651	43.9	21.9
$Fe_3(CO)_7^+ \longrightarrow Fe_3(CO)_4^+$	616	46.4	15.5
$Fe_3(CO)_6^+ \longrightarrow Fe_3(CO)_4^+$	628	45.5	22.8
$Fe_3(CO)_5^+ \longrightarrow Fe_3(CO)_4^+$	628	45.5	45.5

Table VI. Bond Dissociation Energies Measured from Photodissociation Thresholds for $Co_x(CO)_y^+$ Ions

TRANSITION	THRESHOLD		THRESHOLD ENERGY # BONDS BROKEN
	(nm)	(kcal/mole)	(kcal/mole)
$Co_4(CO)_{12}^+ \longrightarrow Co_4(CO)_{10}^+$	640	44.7	22.3
$Co_4(CO)_{11}^+ \longrightarrow Co_4(CO)_9^+$	616	46.4	23.2
$Co_4(CO)_8^+ \longrightarrow Co_4(CO)_6^+$	628	45.5	22.8
$Co_4(CO)_7^+ \longrightarrow Co_4(CO)_5^+$	>651	<43.9	<21.9
$Co_4(CO)_6^+ \longrightarrow Co_4(CO)_4^+$	>651	<43.9	<21.9
$Co_4(CO)_5^+ \longrightarrow Co_4(CO)_3^+$	640	44.7	22.3
$Co_4(CO)_3^+ \longrightarrow Co_4(CO)^+$	640	44.7	22.3
$Co_4(CO)_2^+ \longrightarrow Co_4^+$	628	45.5	22.8
$Co_4^+ \longrightarrow Co_3^+$	604	47.3	15.8[a]
$Co_4^+ \longrightarrow Co_2^+$	>514.5	<55.6	<11.1[a]
$Co_3^+ \longrightarrow Co_2^+$	>514.5	<55.6	<27.8[b]

[a] Tetrahedral structure assumed in calculation of $\bar{D}$(Co–Co). [b] Planar triangular structure assumed in calculation of $\bar{D}$(Co–Co).

is twofold: (i) the transition-metal carbonyl ions have reasonably large absorption cross sections in the visible region, and (ii)

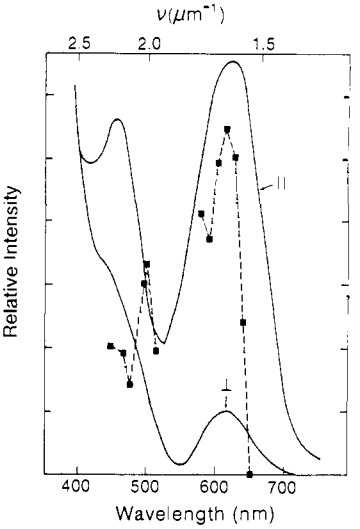

Figure 5. Comparison of (a) the neutral $Fe_3(CO)_{12}$ single-crystal polarized electronic absorption spectrum[44] (solid lines) and (b) the photodissociation spectrum of $Fe_3(CO)_{12}^+$ (dashed line).

metal–metal and metal–carbonyl bond energies are relatively low (<50 kcal/mol (2 eV)). Hence a thermodynamic threshold energy for metal–metal or metal–carbonyl bond dissociation is accessible at energies in the visible spectral region. A general problem in making estimates of bond energies with use of photodissociation thresholds is that the occurrence of photodissociation only provides an upper limit to the bond energy. For example, if the excited state of $M_x(CO)_y^+$ formed by photon absorption lies above the threshold energy for dissociation, the photodissociation threshold is spectroscopically limited. Thus, accurate measurements of bond dissociation energies can only be achieved when an excited electronic state of the ion fortuitously lies close to the dissociation threshold.

It is not possible in our experiment to distinguish a thermodynamic versus a spectroscopic threshold, and no attempt has been made in this work to correct the bond dissociation energies for this anomalous behavior. Thus, we have assumed that at energies above the bond dissociation threshold, the photodissociation spectra for the $M_x(CO)_y^+$ systems are the same as their neutral counterparts (or the molecular ion), and that any deviations from this behavior can be attributed to spectroscopic factors. That is, we have assumed that the chromophore of the $M_x(CO)_y^+$ species is the M_x fragment and that the ligands (or number of ligands) attached to the M_x fragment do not significantly influence the absorption spectrum. Cleary the validity of this assumption will be limited to absorption transitions that are not associated with the ligand or metal–ligand charge-transfer bands. On the basis of Gray's interpretation of the spectroscopic data for $Fe_3(CO)_{12}$, our assumption should be valid. Of course the generality of this assumption will breakdown at some point. For example, Lichtenberger has shown that upon ionization the metal–carbon bond length increases by ca. 0.1 Å for $W(CO)_6$ and ca. 0.14 Å for $Cr(CO)_6$.[45] In metal cluster systems changes in the metal–ligand bonding could result in dramatic changes in the metal–metal bonding, i.e., symmetry changes in the metal center, which could greatly affect the absorption spectrum.[46] It is difficult to systematically study the effects of the metal–ligand ratio on the absorption spectra. However, such effects can be studied by laser–ion beam photodissociation and these studies are currently underway.

A specific example of a photodissociation reaction threshold which can be observed is shown in Figure 5. Figure 5 compares the polarized single-cystal neutral absorption spectrum for $Fe_3(CO)_{12}$ with the photodissociation spectrum for $Fe_3(CO)_{12}^+$. Note

(45) Hubbard, J. L.; Lichtenberger, D. L. *J. Am. Chem. Soc.* **1982**, *104*, 2132.
(46) Manning, M. C.; Trogler, W. C. *Coord. Chem. Rev.* **1981**, *38*, 89.

that the neutral $Fe_3(CO)_{12}$ absorbs at wavelengths greater than 700 nm, but the photodissociation cross section for $Fe_3(CO)_{12}^+$ approaches zero at 651 nm. We attribute the decrease in photofragment ion yield at 651 nm to the energy required for bond cleavage being greater than the energy of the photon, i.e., photodissociation of $Fe_3(CO)_{12}^+$ is thermodynamically limited.

One of the surprising results from Table V is that the photodissociation thresholds for formation of $Fe_3(CO)_4^+$ from $Fe_3(CO)_7^+$ and $Fe_3(CO)_5^+$ are within 1 kcal/mol of each other. One possible explanation is that the measured thresholds correspond to thermodynamic thresholds, which implies that the metal-ligand bonding in $Fe_3(CO)_5^+$ differs from that for $Fe_3(CO)_7^+$. Such an interpretation of the data is consistent with the results from ion-molecule reaction chemistry.[1] On the basis of the reactivities of the ionic cluster fragments, the electron deficiency of the $Fe_3(CO)_7^+$ ion was found to be 3.67 and for $Fe_3(CO)_5^+$ a value of 1.67 was predicted. Such a low value for the electron deficiency of $Fe_3(CO)_5^+$ suggests that the carbonyl ligands may donate more than two electrons to the Fe_3^+ metal center or that the metal-metal bonds in the two ions are different. These questions are presently being investigated further.

Although the single-photon photodissociation of manganese, iron, and cobalt carbonyls has not been studied previously, the gas-phase multi-photon dissociation/ionization (MPD/MPI) of $Mn_2(CO)_{10}$,[47-49] $Fe_3(CO)_{12}$,[50,51] and $Co_4(CO)_{12}$[52] has been reported. In general, the MPD/MPI studies of these metal carbonyl clusters yield bare metal cluster ions. For example, the ions Mn_2^+, Mn^+, Fe_3^+, Fe_2^+, Fe^+, and Co_4^+, Co_3^+, Co_2^+ are the major products observed in the MPD/MPI studies of $Mn_2(CO)_{10}$,[48] $Fe_3(CO)_{12}$,[51] and $Co_4(CO)_{12}$,[52] respectively. One exception to the exclusive production of bare metal ions by MPD/MPI was reported by Lichtin et al.[53] These workers reported the production of carbonyl-containing species such as $Mn_2(CO)_y^+$ (y = 5, 9, 10) and $Mn_3(CO)_y^+$ (y = 8, 10) upon MPD/MPI of $Mn_2(CO)_{10}$. However, these ions were attributed to ion-molecule reactions of Mn^+ with various neutrals of the type $Mn_2(CO)_y$ (formed by MPD) and not from the direct dissociation/ionization of the neutral. The removal of all carbonyl ligands from $Mn_2(CO)_{10}$ as well as ionization of the bare metal neutrals is thought to require between seven and ten photons in the 350-450 nm range.

The results presented here also find the same bare metal cluster ions produced as a result of single-photon photodissociation. The difference is, however, that we are photodissociating mass selected ions, e.g., Mn_2^+ arises from the photodissociation of $Mn_2(CO)_y^+$ (y = 1-5) and not from $Mn_2(CO)_{10}^+$. The fact that only Mn_2^+ and Mn^+ ions are observed in the MPI mass spectra of $Mn_2(CO)_{10}$ suggests that the Mn-Mn bond strength must be greater than the Mn-CO bond strength. Of course, another critical difference between the MPD/MPI and single-photon photodissociation studies is the photon wavelength. The wavelength used for photoactivation could be important, especially if metal-ligand charge-transfer bands are populated in the ultraviolet range. The single-photon photodissociation results differ in that cleavage of the Mn-Mn bond is possible and $Mn(CO)_y^+$ product ions are observed (see Table I). For example in Figure 2, the photodissociation cross section for $Mn_2(CO)_{10}^+ \rightarrow Mn(CO)_5^+$ is quite large even at low energy (581-651 nm), a result that suggests that the Mn-Mn bond in $Mn_2(CO)_{10}^+$ is weak. Other differences between the MPD/MPI and the single-photon photodissociation studies could be attributed to the fact that the dissociation energy of the Mn-Mn bond in $Mn_2(CO)_y^+$ type ions differs from that of the neutral molecule. For example, ionization of $Mn_2(CO)_{10}$ is thought to occur from a molecular orbital with large amounts of metal character.[54,55]

Table VII. Comparison of $\bar{D}$(M-M) and $\bar{D}$(M-CO) Obtained from the Literature and Those Obtained by the Laser-Ion Beam Photodissociation Technique Presented in This Paper (All Values Are Reported in kcal/mol)

	M = Mn		M = Fe		M = Co	
	lit.	this work	lit.	this work	lit.	this work
$\bar{D}$(M-CO)	24[a]	<25.0	27.7[b]	23.9	34[c]	22.6
$\bar{D}$(M-M)	32[d]	<43.9	27-50[e]		22[a]	15.8

[a] See ref 58. [b] See ref 24. [c] See ref 71. [d] See ref 56 and 60. [e] See ref 27.

$Mn_2(CO)_{10}$ is by far the most intensely studied metal carbonyl system. Numerous reports on the Mn-Mn bond energy in $Mn_2(CO)_{10}$ derived from gas- and solution-phase studies have been reported. The values for the bond dissociation energy of Mn-Mn vary from 22[56] to 41 ± 9[57] kcal/mol. There are fewer reports on the average Mn-CO bond dissociation energy, and the value of 24 kcal/mol reported by Connor et al. is generally accepted.[58] The metal-metal bond energy in $Mn_2(CO)_{10}^+$ has been reported to be 32.2 kcal/mol,[56] while that of Mn_2^+ varies from 19.6 ± 5[59] to ≥32.0 kcal/mol.[60] Because most $Mn_x(CO)_y^+$ ions photodissociate at wavelengths greater than 651 nm, accurate energy thresholds cannot be obtained from the data of Table IV. But on the other hand, upper limits for the Mn-CO and Mn-Mn bond dissociation energies can be made. Bond dissociation energies derived from single-photon photodissociation thresholds for homolytic Mn-Mn bond cleavage of $Mn_2(CO)_{10}^+$ and Mn_2^+ precursor ions (Table IV) were both found to be <43.9 kcal/mol. One of the surprising results from the data in Table IV is that $Mn_2(CO)_5^+$ is formed by photodissociation of $Mn_2(CO)_{10}^+$. This process yields an extremely low value for the average Mn-CO bond dissociation energy, viz., <8.8 kcal/mol. Appearance potential measurements for the loss of five carbonyl ligands from $Mn_2(CO)_{10}^+$ yields an average Mn-CO bond energy of 15.4 kcal/mol,[61] an equally surprising low value for the metal-ligand bond energy. At first it was thought that removal of five carbonyl ligands from the molecular ion must occur by a multiphoton process. However, photodissociation experiments performed with a perpendicular laser-ion beam configuration in the third field free region of the mass spectrometer, where the interaction time between ion and laser beam is very short, i.e., <1 ns, are inconsistent with a multiphoton process occurring.

In Table VII we have compared average metal-metal and metal-carbonyl bond dissociation energies reported in this paper with available literature values. Most of the measured bond energies listed in Table VII are substantially lower than the average bond dissociation energies taken from the literature. One possible explanation for this is that many of the manganese, iron, and cobalt carbonyl ions do not photodissociate at wavelengths greater than 581 nm and must reach threshold at wavelengths between 514.5 and 581 nm. Therefore, when the bond dissociation energies for all the photodissociating ions are considered, the calculated average bond dissociation energy may indeed be larger. Another possibility is that the ions possess some excess rovibronic energy that reduces the photodissociation threshold, thus lowering

(47) Rothberg, L. J.; Gerrity, D. P.; Vaida, V. *J. Chem. Phys.* **1981**, *74*, 2218.
(48) Leopold, D. G.; Vaida, V. *J. Am. Chem. Soc.* **1984**, *106*, 3720.
(49) Kobayashi, T.; Ohtani, H.; Noda, H.; Teratani, S.; Yamazaki, H.; Yasufuku, K. *Organometallics* **1986**, *5*, 110.
(50) Welch, J. A.; Vaida, V.; Geoffroy, G. L. *J. Phys. Chem.* **1983**, *87*, 3635.
(51) Leutwyler, S.; Even, U. *Chem. Phys. Lett.* **1981**, *84*, 188.
(52) Hollingsworth, W. E.; Vaida, V. *J. Phys. Chem.* **1986**, *90*, 1235.
(53) Lichtin, D. A.; Bernstein, R. B.; Vaida, V. *J. Am. Chem. Soc.* **1982**, *104*, 1830.
(54) Levenson, R. A.; Gray, H. B. *J. Am. Chem. Soc.* **1975**, *97*, 6042.
(55) Green, J. C.; Mingos, D. M. P.; Seddon, E. A. *Inorg. Chem.* **1981**, *20*, 2595.
(56) Connor, J. A.; Zafarani-Moattar, M. T.; Bickerton, J.; El Saied, N. I.; Suradi, S.; Carson, R.; Al Takhin, G.; Skinner, H. A. *Organometallics* **1982**, *1*, 1166.
(57) Martinho Simões, J. A.; Schultz, J. C.; Beauchamp, J. L. *Organometallics* **1985**, *4*, 1238.
(58) Connor, J. A.; Skinner, H. A.; Virmani, Y. *Faraday Symp. Chem. Soc.* **1984**, *8*, 18.
(59) Ervin, K.; Loh, S. K.; Aristov, N.; Armentrout, P. B. *J. Phys. Chem.* **1983**, *87*, 3593.
(60) Jarrold, M. F.; Illies, A. J.; Bowers, M. T. *J. Am. Chem. Soc.* **1985**, *107*, 7339.
(61) Svec, H. J.; Junk, G. A. *J. Am. Chem. Soc.* **1967**, *89*, 2836.

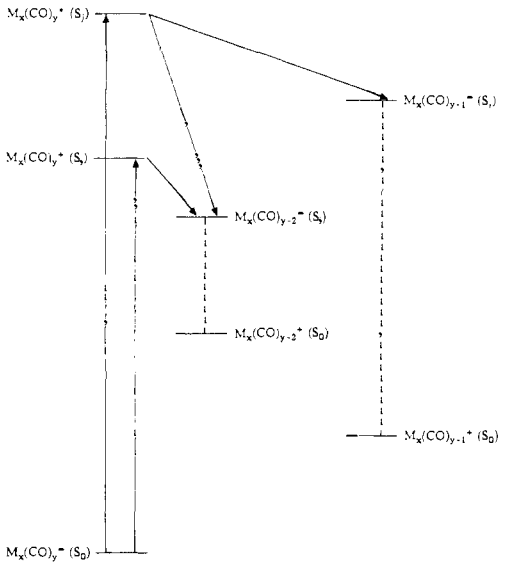

Figure 6. Mechanism demonstrating how loss of two carbonyls at longer wavelengths and loss of one and two carbonyls at shorter wavelength may occur when the excited states of the photoproducts are accessed.

the measured bond dissociation energy. For example, the bond energy of Mn_2^+ determined by collision-induced dissociation is 0.85 ± 0.2 eV,[59] whereas the photodissociation data give a value of ≥ 1.39 eV.[60] A possible explanation for the differences in the dissociation energies for Mn_2^+ is the excess internal energy of the ion in the study reported by Armentrout.

It is not surprising that ionic metal species are formed with excess energy. Photolysis experiments on $Mn_2(CO)_{10}^+$ ($\lambda = 351$ nm) suggest that $Mn(CO)_5$ is produced in excited vibrational states, which undergo radiative decay to the ground electronic state by emission of a red photon.[62] The single-photon[63] and multiphoton[64] ionization of $Fe(CO)_5$ have produced iron atoms in excited electronic states. Yardley et al. recently reported that the laser photodissociation of $Fe(CO)_5$ yielded $Fe(CO)_{5-n}$ ($1 \leq n \leq 4$) neutrals with retention of internal energy.[65] It is, however, surprising that the authors found even the small neutrals (e.g., Fe(CO) and $Fe(CO)_2$) contained excess internal energy because loss of CO neutrals is thought to be effective in removing excess energy.[66] Likewise, laser photolysis/transient infrared studies of $Fe(CO)_5$[67,68] and $Cr(CO)_6$[69] demonstrate that the photoproducts have infrared stretching bands that blue shift with time and reach a fixed maximum stretching frequency within a time period of 10 μs. A long-lived excited state of Cr^+ was also invoked to explain the different kinetic data for reactions of Cr^+ formed by direct electron impact ionization of $Cr(CO)_6$.[70] Ridge et al. proposed that 25% of the Cr^+ ions had reaction rates 4.4 times larger than the remaining Cr^+ ions.

One aspect of the photodissociation data that cannot be attributed to excess energy of the ion is the loss of multiple CO ligands at high energies and the exclusive loss of two CO ligands at low photon energy. Although such trends could be attributed to state-specific reactions, we prefer to rationalize the data in more general terms. Figure 6 illustrates why specific reactions may occur at low photon energy and other reaction channels requiring less energy may not. At high energies the higher lying excited electronic state (S_j) of $M_x(CO)_y^+$ can be accessed, and photodissociation yields excited state (S_i) product ions $M_x(CO)_{y-1}^+$ and $M_x(CO)_{y-2}^+$. However, at low energies, only the low-energy excited state of $M_x(CO)_y^+$ is formed (S_i), and S_i dissociates to yield excited-state species of $M_x(CO)_{y-2}^+$. Although the ground-state energy of $M_x(CO)_{y-2}^+$ is greater than the ground-state energy of $M_x(CO)_{y-1}^+$, photofragmentation of these ions may occur by specific electronic transitions which lead exclusively to the loss of two carbonyl ligands at low energy.

Although state-specific reactions of large polyatomic systems are rare, such behavior is feasible and even quite probable for transition-metal systems. The vibrational modes of the metal centers of cluster fragments are not effectively coupled with other modes of the molecule. That is, the low vibrational frequencies of the metal centers could reduce the rates for energy randomization into other degrees-of-freedom. In order to probe these ideas further studies are presently underway to ascertain the effects of different excited states on the photodissociation process. In particular, further work will concentrate on the efficiency of photodissociation via metal–ligand charge-transfer bands, and these reactions will be compared with photodissociation via metal–metal bonding electronic states.

Acknowledgment. This work was supported by grants from the U.S. Department of Energy, Office of Basic Energy Sciences (DE-AS05-82ER13023), and the National Science Foundation (CHE-8418457).

Registry No. $Mn_2(CO)_{10}$, 10170-69-1; $Fe_3(CO)_{12}$, 17685-52-8; $Co_4(CO)_{12}$, 17786-31-1.

(62) Bray, R. G.; Seidler, P. F.; Gethner, J. S.; Woodin, R. L. *J. Am. Chem. Soc.* **1986**, *108*, 1312.
(63) Horák, D. V.; Winn, J. S. *J. Phys. Chem.* **1983**, *87*, 265.
(64) Nagano, Y.; Achiba, Y.; Kimura, K. *J. Chem. Phys.* **1986**, *84*, 1063.
(65) Yardley, J. T.; Gitlin, B.; Nathanson, G.; Rosan, A. M. *J. Chem. Phys.* **1981**, *74*, 370.
(66) Jarrold, M. F.; Misev, L.; Bowers, M. T. *J. Phys. Chem.* **1984**, *88*, 3928.
(67) Seder, T. A.; Ouderkirk, A. J.; Weitz, E. *J. Chem. Phys.* **1986**, *85*, 1977.
(68) Ouderkirk, A. J.; Seder, T. A.; Weitz, E. *Applications of Lasers to Industrial Chemistry*; SPIE-The International Society for Optical Engineering: Bellingham, Washington, 1984; Vol. 458, p 148.
(69) Seder, T. A.; Church, S. P.; Weitz, E. *J. Am. Chem. Soc.* **1986**, *108*, 4721.
(70) Reents, W. D., Jr.; Strobel, F.; Freas, R. B., III; Wronka, J.; Ridge, D. P. *J. Phys. Chem.* **1985**, *89*, 5666.
(71) Baev, A. K. *Russ. J. Phys. Chem.* **1980**, *54*, 1.